Molecular and Cellular Endocrinology 512 (2020) 110854

Contents lists available at ScienceDirect

Molecular and Cellular Endocrinology

journal homepage: www.elsevier.com/locate/mce

Time course of photo-induced Egr-1 expression in the hypothalamus of a seasonally breeding songbird

Donna L. Maney[a,*], Robert A. Aldredge[b], Shaquille H.A. Edwards[a], Nathan P. James[a], Keith W. Sockman[b]

[a] Department of Psychology, Emory University, Atlanta, GA, USA
[b] Department of Biology, University of North Carolina, Chapel Hill, NC, USA

ARTICLE INFO

Keywords:
Egr-1
Dopamine
Gonadotropin-releasing hormone
Tyrosine hydroxylase
Vasoactive intestinal peptide
White-throated sparrow

ABSTRACT

Many seasonally-breeding species use daylength to time reproduction. Light-induced release of progonadal hormones involves a complex cascade of responses both inside and outside the brain. In this study, we used induction of early growth response 1 (Egr-1), the protein product of an immediate early gene, to evaluate the time course of such responses in male white-throated sparrows (*Zonotrichia albicollis*) exposed to a single long day. Induction of Egr-1 in the pars tuberalis began ~11 h after dawn. This response was followed ~6 h later by dramatic induction in the tuberal hypothalamus, including in the ependymal cells lining the third ventricle. At approximately the same time, Egr-1 was induced in dopaminergic and vasoactive intestinal peptide neurons in the tuberal hypothalamus and in dopaminergic neurons of the premammillary nucleus. We noted no induction in gonadotropin-releasing hormone (GnRH) neurons until 2 h after dawn the following morning. Overall, our results indicate that Egr-1 responses in GnRH neurons occur rather late during photostimulation, compared with responses in other cell populations, and that such induction may reflect new synthesis related to GnRH depletion rather than stimulation by light cues.

1. Introduction

In seasonally-breeding species, reproduction must be timed to coincide with peak availability of resources to care for offspring. Among all available cues that can indicate approaching spring, such as ambient temperature, plant growth, and food availability, celestial cues are the most reliable. Most seasonally breeding birds use daylength as a cue to initiate gonadal recrudescence and the onset of reproduction (Wingfield and Kenagy, 1991). As daylength increases in the spring, it eventually reaches a threshold that triggers release of gonadotropin releasing hormone I (hereafter referred to as GnRH) from the median eminence, thus stimulating secretion of luteinizing hormone (LH) and follicle stimulating hormone and, in turn, gonadal development and secretion of sex steroids. At sub-threshold daylengths, other types of cues are unlikely to cause the initiation of gonadal development in birds. Even in temporally flexible species that depend on additional cues, lengthening days are nonetheless also required (Deviche and Small, 2001). Daylength is thus a critical piece of information that must be transduced effectively and efficiently.

The avian photoperiodic response, in other words the transduction of long daylength into an endocrine response, has most often been studied in captive populations in order to precisely manipulate photoperiod and the time of dawn, to which circadian rhythms are entrained. In a popular experimental procedure that has been called the "first long day" paradigm (Meddle and Follett, 1997; Hanon et al., 2008; Majumdar et al., 2014), birds in non-breeding condition are transferred abruptly from a short, winter-like photoperiod to a long, spring-like one. In an early study of Japanese quail (*Coturnix coturnix japonica*), a single long day caused an increase in plasma LH that was detectable well before dawn the following day (Nicholls and Follett, 1974). Subsequent studies demonstrated the same rapid LH response in white-crowned sparrows (*Zonotrichia leucophrys*; Follett et al., 1974). Thus, the hormonal component of the photoperiodic response can occur quite rapidly. The neural responses that lead to GnRH release must therefore be happening even earlier.

Over the past two decades, intense experimentation on the early stages of the photoperiodic response has revealed a complex sequence of events involving multiple structures inside and outside the brain. The mechanisms that underlie the response are largely consistent with an elegant model originally proposed in the 1930's by Bünning (see

* Corresponding author.
E-mail address: dmaney@emory.edu (D.L. Maney).

https://doi.org/10.1016/j.mce.2020.110854
Received 1 November 2019; Received in revised form 25 April 2020; Accepted 28 April 2020
Available online 16 May 2020
0303-7207/

Bünning, 1960). According to the "external coincidence model", a circadian rhythm in photosensitivity persists year round, with peak sensitivity in the evening. As spring approaches and days grow longer, light eventually coincides with the peak in sensitivity, triggering an endocrine response. Contemporary research has confirmed that it is not the duration of light during the day, but timing of light, which is stimulatory in the evening, that initiates the response. Clock genes, such as *Per2*, *Per3*, and *Bmal1*, are expressed in the mediobasal hypothalamus in a variety of avian species (Leclerc et al., 2010; Perfito et al., 2012; Yasuo et al., 2003), often in or in proximity to cells expressing photopigments such as melanopsin, neuropsin, or VA-opsin (reviewed by García-Fernández et al., 2015; Pérez et al., 2018), providing a potential molecular substrate for the detection of light at particular times of day.

Downstream of cells that tell time and detect light, the steps leading to GnRH release in birds is thought to be similar to that in mammals (Korf, 2018). This process has been recently reviewed by others (e.g., Nakane and Yoshimura, 2019). Briefly, a signal is transmitted to the pars tuberalis (PT) of the pituitary, which lies immediately ventral to the median eminence of the hypothalamus. In response, PT secretes thyroid stimulating hormone (TSH), which travels a short distance to the tanycytes lining the third ventricle (vIII). The tanycytes (also called ependymal cells) in turn increase their production of the thyroid hormone–activating enzyme type 2 deiodinase, which increases production of triiodothyronine (T3). The T3 acts on the glial cells that encase the terminals of GnRH neurons at the median eminence, causing their endfeet to retract. This anatomical change allows the GnRH terminals to come into contact with the portal vasculature. The entire process occurs in a matter of hours, leading to LH release by about 18 h after dawn (Meddle and Follett, 1997).

Compared with the large number of other cell types involved in the avian photoperiodic response, the GnRH neurons themselves are thought to play a relatively passive role. Photostimulation does not always increase hypothalamic GnRH or the number of GnRH neurons (Dawson et al., 1985; Foster et al., 1987; Saldanha et al., 1994; Meddle et al., 2006) even though the demand for GnRH presumably increases rapidly. Photostimulation failed to induce immediate early gene (IEG) expression in GnRH somata in mallards (*Anas platyrhynchos*; Péczely and Kovács, 2000) and Japanese quail (Meddle and Follett, 1997) although it did induce IEG expression in the mediobasal hypothalamus around the GnRH terminals (Meddle and Follett, 1997). LH release induced by injection of N-methyl-D-aspartate (NMDA) was accompanied by IEG expression in the mediobasal hypothalamus, but not in the GnRH somata, in white-crowned sparrows (Meddle et al., 1999), white-throated sparrows (*Z. albicollis*; Maney et al., 2007), rufous-crowned sparrows (*Aimophila ruficeps*; Deviche et al., 2008) and Cassin's sparrows (*Aimophila cassinii*; Deviche et al., 2008). In great tits (*Parus major*), photo-induced LH secretion *preceded* the increase in GnRH mRNA (Perfito et al., 2012). Together, these results suggest that GnRH release, photo-induced or otherwise, does not require new transcription or protein synthesis in the GnRH neurons themselves. This model is consistent with findings in rodents that the LH surge happens before, not after, induction of IEGs in GnRH somata (Doan et al., 1994) and that NMDA elicits LH release without concomitant induction of IEGs in those cells (Ebling et al., 1993; Lee et al., 1993).

Despite the above evidence that GnRH release is not accompanied by IEG induction in GnRH somata, we showed previously that in white-throated sparrows, a single long day induced expression of the IEGs Fos and early growth response protein (Egr-1) in GnRH immunoreactive (IR) neurons of the preoptic area (Saab et al., 2010). Further, the magnitude of this Egr-1 response was significantly positively correlated with plasma LH levels. In that study, we sampled both brain tissue and plasma between 26 and 27 h after dawn of the first long day, and all photostimulated birds showed colocalization of Egr-1 and GnRH-IR. Thus, we could not determine the exact time at which the Egr-1 response in GnRH neurons began. A major goal of the current study was therefore to determine the earliest time point at which we could detect Egr-1 responses in GnRH neurons of the preoptic area.

In our previous study (Saab et al., 2010) we detected Egr-1 immunoreactivity (ir) not only in the GnRH neurons of the preoptic area, but also in cells of largely unknown phenotype throughout the mediobasal hypothalamus (see Maney et al., 2007). A second major goal of the current study was thus to determine the phenotypes of some of these cells and to track the time course of their responses.

In white-throated sparrows, the most dramatic Egr-1 response to photostimulation in the brain occurs in the infundibular region (see Maney et al., 2007). We therefore investigated the extent to which these responding cells are immunopositive for vasoactive intestinal peptide (VIP), a neuropeptide synthesized in the infundibular region in this species (Horton et al., 2020; Maney et al., 2005) and which is a releaser of prolactin (Macnamee et al., 1986; Maney et al., 1999a). Like LH, prolactin is released at the beginning of the breeding season in response to long days and is thought to be pro-gonadal in the very early stages of breeding (Hiatt et al., 1987; Maney et al., 1999b). The prolactin response is thought to be delayed, however, compared with the LH response (El Halawani et al., 2009; Sharp, 2005), and other researchers have not observed photo-induced increases in VIP mRNA or IEG induction in this VIP cell population (Li & Kuenzel et al., 2008; Thayananuphat et al., 2007b). In this study, we tested for such induction and also characterized its time course.

We were also interested in the responding cells located caudal to the median eminence, at the juncture between the mediobasal hypothalamus and the midbrain. In turkeys, much attention has focused on the premammillary nucleus, located in this area, which contains the A11 group of dopaminergic neurons (Kuenzel and Masson, 1988; Reiner et al., 1994). These neurons express the dopamine-synthetic enzyme tyrosine hydroxylase (TH) and melatonin in a circadian rhythm, with TH highest during the day and melatonin at night (Kang et al., 2010). The cells are also photoreceptive, and have been proposed to carry information on daylength to the median eminence where they release dopamine, causing the PT to secrete TSH (Kang et al., 2010). This dopamine could also affect VIP release (Bhatt et al., 2003; Chaiseha et al., 1997), which in turn could affect prolactin secretion. Here, we tested for Egr-1 induction in these TH-IR cells and tracked the time course of these responses.

In summary, our primary goal in the present study was to characterize the time course of Egr-1 responses in white-throated sparrows throughout the evening and night of the first long day. By colocalizing Egr-1-ir with GnRH-ir, TH-ir or VIP-ir, we sought to gain information about the phenotypes of the responding cells and to determine the order in which these responses occur. Beginning at 10 h after dawn and continuing at regular intervals until 26 h, we looked for Egr-1 induction in GnRH-IR somata, the PT, the mediobasal hypothalamus (in particular the tanycytes lining vIII), and the TH-IR and VIP-IR cells of the tuberal hypothalamus and premammillary nucleus. In so doing, we aimed to determine the time at which each cell type begins to express Egr-1, relative to the other regions, during photostimulation. In this way we sought a more complete characterization of the sequence of events than what was previously possible by sampling at a single time point.

2. Methods

2.1. Experiment 1

2.1.1. Manipulation of photoperiod

White-throated sparrows (n = 36 males) were collected during autumn migration in Chapel Hill, NC USA and housed at the University of North Carolina. Sex was determined by PCR analysis of a blood sample (Griffiths et al., 1998). They were initially housed in aviaries in two separate rooms for 17–18 weeks. The lights came on each day at 7:00 a.m., which we refer to as Zeitgeber time (ZT) 0, and went out at 3:00 p.m., or ZT8. Thus, the daylength during this period was 8 h of light and 16 h of dark (8 L:16D). In mid-January, the birds were transferred to

sound-attenuated chambers (18 chambers) with two animals per chamber. White-throated sparrows occur in two plumage morphs that differ with respect to some features of their neuroendocrinology (Horton et al., 2014; Lake et al., 2008; Maney et al., 2005); we balanced morph in the study by housing one bird of each morph inside each chamber. The light cycle for each chamber was individually controlled by a timer and was the same as in the aviaries (8 L:16D, same on/off times). After a one-week acclimation period inside the chambers, the lights for half of the chambers (9 chambers, 18 birds) were plugged into a constant power source until 11:00 p.m. (ZT16) such that those chambers received 16 h of light. We refer to those birds below as long-day (LD). The other chambers remained on 8 L and we refer to those birds as short-day (SD). We spatially interspersed individual LD chambers with individual SD chambers, allowing us to statistically treat each chamber as an independent experimental unit relative to the photoperiod treatment. The lights in the main room that housed the chambers went off at ZT8 as usual and remained off until ZT0 the next day.

2.1.2. Tissue collection

We collected brains from 6 LD and 6 SD animals during each of three 1.5 h intervals (Fig. 1). The first interval occurred between 5:30 p.m. and 7:00 p.m., in other words 10.5–12 h after dawn. For simplicity, we will refer to this group as Zeitgeber time ZT11 even though it contained a range of ZTs spanning 1.5 h. The second interval occurred between 1:00 a.m. and 2:30 a.m., which we refer to as ZT19. The third interval occurred the following morning between 8:00 a.m. and 9:15 a.m. and we refer to it as ZT26. Note that ZT26 is the same as ZT2 the following day; we opted to use the term ZT26 in order to avoid confusion about the sequence of sampling. All three of these sampling intervals occurred before the earliest samples in our previous study (Saab et al., 2010); in the current study, the latest sampling time was ZT26.0, whereas in our previous study, the first bird was sampled at ZT26.1. For both the ZT11 and ZT19 time points, we entered the animal room with a flashlight to collect the animals from the chambers. At all time points, both of the birds within a given chamber were collected. Each bird was rapidly decapitated within 1 min of removing it from its chamber. The brains were immediately dissected from the skulls and fixed in 5% acrolein (see Saab et al., 2010). They were washed in PBS, cryoprotected in 30% sucrose, frozen in powdered dry ice, and shipped to Emory University, Atlanta, GA USA. To verify non-breeding reproductive condition, we inspected the testes at the time of sacrifice. Testes were regressed in all birds.

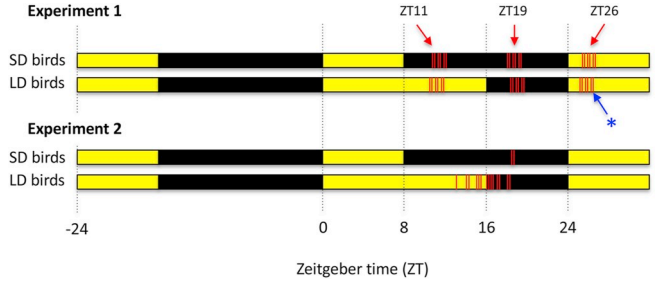

Fig. 1. Design of the two experiments. Each horizontal bar represents a group of birds and their light cycle (yellow = lights-on; black = lights-off). All birds were housed on 8 L:16D for at least 10 weeks before the start of the study. The last 8 h day before the experiment is shown on the left side of the figure (24 h before dawn on the day of the experiment). At Zeitgeber time (ZT) 0, the lights came on as usual for all of the birds. For short-day (SD) birds (top bar in each pair), the lights went out as usual at 8 h after dawn. For the long-day (LD) birds, the lights remained on until 16 h after dawn. The following morning, the lights came on at the usual time (Experiment 1 only). Each vertical red line denotes one bird sampled at that time. "ZT11" spanned ZT 10.5–12 (n = 6 LD, 6 SD); "ZT19" spanned ZT 18–19.5 (n = 6 LD, 6 SD); "ZT26" spanned ZT 25–26.25 (n = 6 LD, 6 SD). *The blue asterisk indicates the last LD bird, which was the only bird in which GnRH-IR cells were seen to co-express Egr-1-IR in the entire study, see Fig. 2.

2.1.3. Immunohistochemistry

Immunohistochemistry was conducted on free-floating 50 μm sections. Brains were cut on a microtome, in the coronal plane, into two series of alternate sections. Sections were stored at −20 °C in cryoprotectant until use. The immunohistochemical procedures to label GnRH, Egr-1, VIP, and TH are described below. All assays were done using the ABC method, in other words using biotinylated secondary antibodies (all anti-rabbit raised in goat, except for TH, which uses anti-mouse raised in goat) and the Vectastain Elite kit (Vector, Burlingame, CA USA). Our protocols for labeling each of the antigens have been previously published, and those references are noted below. The assays were run in batches with treatment (LD or SD) and time point (evening, night, or morning) balanced across batch. At the end of each assay, sections were mounted on subbed microscope slides and coverslipped in DPX.

2.1.4. Egr-1 + GnRH immunolabeling

Sections containing the preoptic area from one series were double-labeled for Egr-1 and GnRH as described by Saab et al. (2010). The anti-Egr-1 antibody (Santa Cruz Biotechnology cat. #sc189; Santa Cruz, California, USA) was diluted 1:8000 for labeling, and was visualized using diaminobenzidine enhanced with nickel. The anti-GnRH antibody [HU60, donated by H. Urbanski (Oregon Health and Science University, Beaverton, OR, USA)] was diluted 1:5000 for labeling and was visualized using diaminobenzidine. Each of these antibodies was previously validated in brain tissue from white-throated sparrows using the procedure of Saper and Sawchenko (2003). All specific staining was abolished by pre-incubating the antibody with Egr-1 or GnRH peptide (Saab et al., 2010).

We inspected all GnRH-IR neurons in each 50-μm section in an area bounded rostrally by the first appearance of the septo-mesencephalic tract and caudally by the pallial commissure (Fig. 2). This area encompasses the majority of ME-projecting GnRH neurons in passerines (Stevenson et al, 2012) and contains the population in which Egr-1 induction at ZT26-27 predicts plasma LH levels (Saab et al., 2010). We made note of all double-labeled cells, in other words cells in which GnRH-ir and Egr-1-ir were colocalized, throughout this region as well as in the lateral septum. All cell counting was done by observers blind to the experimental group.

2.1.5. Egr-1 + TH immunolabeling

One series of alternate sections caudal to the preoptic area, containing the hypothalamus and rostral midbrain, was double-labeled for Egr-1 and TH as previously described (LeBlanc et al., 2007). As above, the anti-Egr-I antibody was diluted 1:8000 and visualized using diaminobenzidine enhanced with nickel. The anti-TH antibody (ImmunoStar Cat. no. 22941) was diluted 1:10,000 and visualized using diaminobenzidine. See Matragrano et al. (2011) for a discussion of the validation of the anti-TH antibody in birds. Sections were mounted onto microscope slides and coverslipped in DPX.

The labeled sections were inspected to assess Egr-1 induction within the PT and tuberal hypothalamus, particularly around vIII (Fig. 3). Egr-1 induction was determined subjectively on a scale of 0–4, with 0 corresponding to no induction and 4 corresponding to extremely dense Egr-1 labeling. As part of a previous study, we compared subjective ratings with the estimation of labeling density determined using ImageJ (NIH) thresholding and found the two methods to be comparable with respect to inter-rater reliability and ability to detect effects (L. Matragrano and D. Maney, unpublished). All observations were made blind to the experimental group. The TH labeling did not mask the Egr-1 labeling.

TH-IR cells were counted in two areas of the mediobasal hypothalamus: the tuberal hypothalamus (Fig. 4) and the premammillary

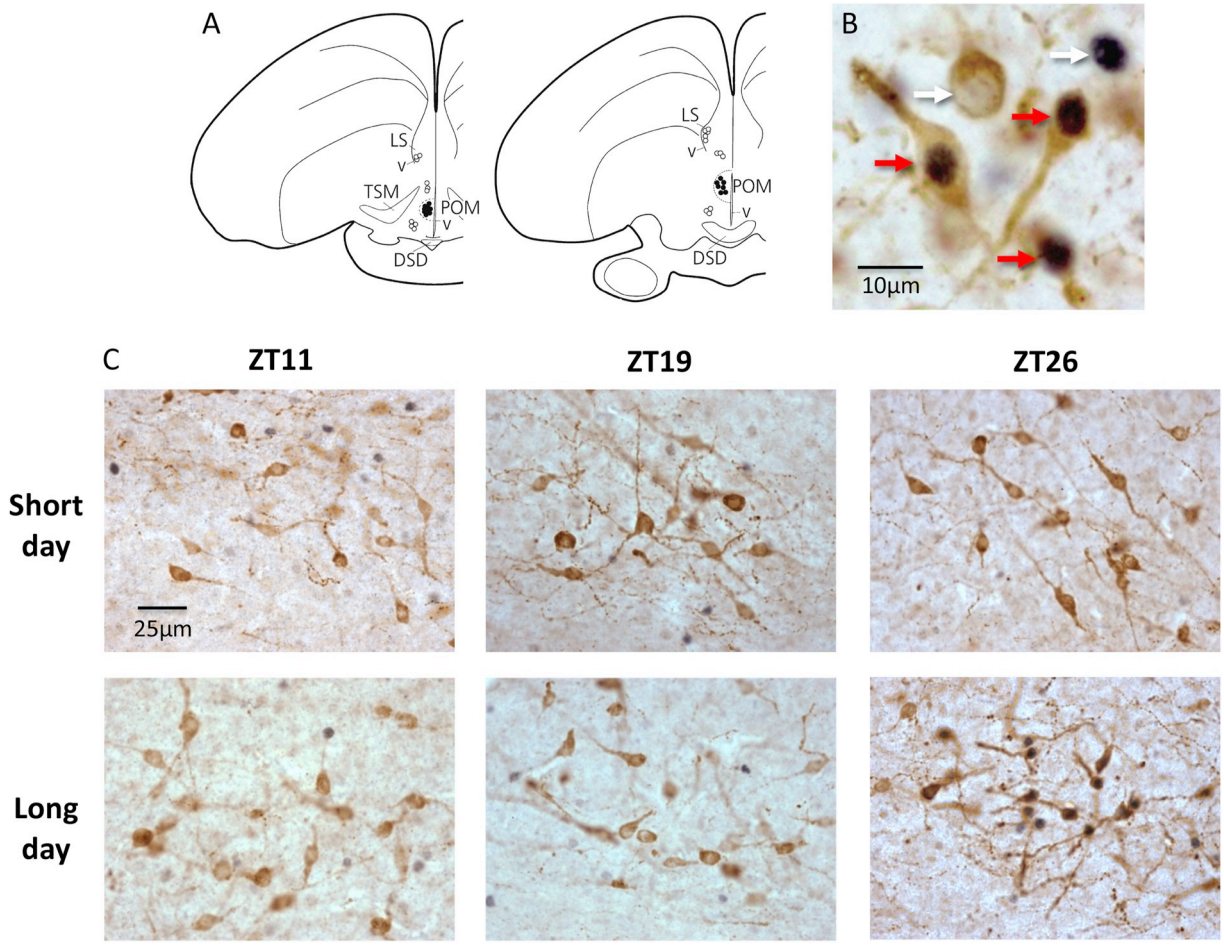

Fig. 2. Photo-induced Egr-1 immunoreactivity (ir) in gonadotropin releasing hormone (GnRH) immunoreactive (IR) neurons (Experiment 1). (A) Coronal sections showing the distribution of GnRH-IR cells (filled circles) in which Egr-1-ir was induced by long day length at Zeitgeber time (ZT) 26. Cells represented by white circles did not express Egr-1-ir. (B) Neurons single-labeled for GnRH only or Egr-1 only (white arrows), or double-labeled for both GnRH and Egr-1 (red arrows). The GnRH-ir is reddish brown, and the Egr-1-ir is purplish gray. (C) We noted no double-labeling in any of the brains at ZT11 or ZT19 and Egr-1-ir was induced by photostimulation in only one out of the six LD birds at ZT26 (see Fig. 1). The scale bar applies to all panels in (C). DSD, supraoptic decussation. LS, lateral septum. POM, medial preoptic area. TSM, septomesencephalic tract. v, ventricle.

nucleus (PMM; Fig. 5). These populations likely correspond to portions of the A12 and A11 cell groups, respectively (Kuenzel and Masson, 1988; Kabelik et al., 2011; Reiner et al., 1994; Roberts et al., 2001). Note that some researchers have argued that the A12 population is absent in birds (Appeltants et al., 2001), whereas others have assigned the tuberal population to A12 (Kabelik et al., 2011; Reiner et al., 1994; Roberts et al., 2001). The cells we counted in the tuberal hypothalamus were located at the base of the brain (Fig. 4), lateral and ventral to vIII and dorsal to the median eminence, within the boundaries of the photo-induced Egr-1 response (Maney et al., 2007). It is possible that at least some of the TH-IR neurons we counted could have been part of a ventral A14 cell group (see Reiner et al., 1994). A separate population of TH-IR neurons, located lateral and dorsal to vIII, has been referred to as the dorsolateral A12 cell group (Kabelik et al., 2011). This group was not included in these counts because we never noted Egr-1-ir in those cells. For each group of TH-IR cells counted (the tuberal hypothalamus and PMM) we noted the number of those cells co-expressing Egr-1-ir (Figs. 4 and 5). All cell counting was done by observers blind to the experimental group.

2.1.6. *Egr-1 + VIP immunolabeling*

One series of alternate sections caudal to the preoptic area, containing the hypothalamus and rostral midbrain, was double-labeled for Egr-1 and VIP. Immunohistochemistry for Egr-1 and VIP was performed following the method of Maney et al. (2008). As above, the anti-Egr-1 antibody was diluted 1:8000 and visualized using diaminobenzidine enhanced with nickel. The anti-VIP antibody (Immunostar Cat. No. 20077) was diluted 1:10,000 and visualized using diaminobenzidine (see Maney et al., 2008). Ball et al. (1988) showed that in song sparrows (*Melospiza melodia*) all specific staining is abolished by preadsorbing the primary antibody with synthetic peptide for 8 h prior to tissue incubation.

VIP-IR cells were counted in the same two areas in which TH-IR cells were counted, the tuberal hypothalamus (Fig. 6) and PMM (Fig. 7). Both of these VIP cell populations have been well-described in birds (Deviche et al., 2000; Saldanha et al., 1994; Sharp, 2005; Wang and Wingfield, 2011; Zhao et al., 2018). By overlaying alternate sections labeled for either VIP or TH, we determined that within the PMM, the VIP-IR cells and TH-IR cells were close together but not overlapping. The VIP cell population was slightly dorsal and lateral to the TH population (Fig. 7A). For both the tuberal hypothalamus and PMM, as above, we noted the number of cells co-expressing Egr-1-ir. All cell counting was done by observers blind to the experimental group.

Induction of Egr-1 in the tuberal hypothalamus and PT was inspected in the VIP-labeled series as described for the TH-labeled series above, as a check that our assessment of induction in each brain was repeatable. The assessments made from the VIP series (scale of 0–4, see Fig. 3) matched that made from the TH series in almost every case.

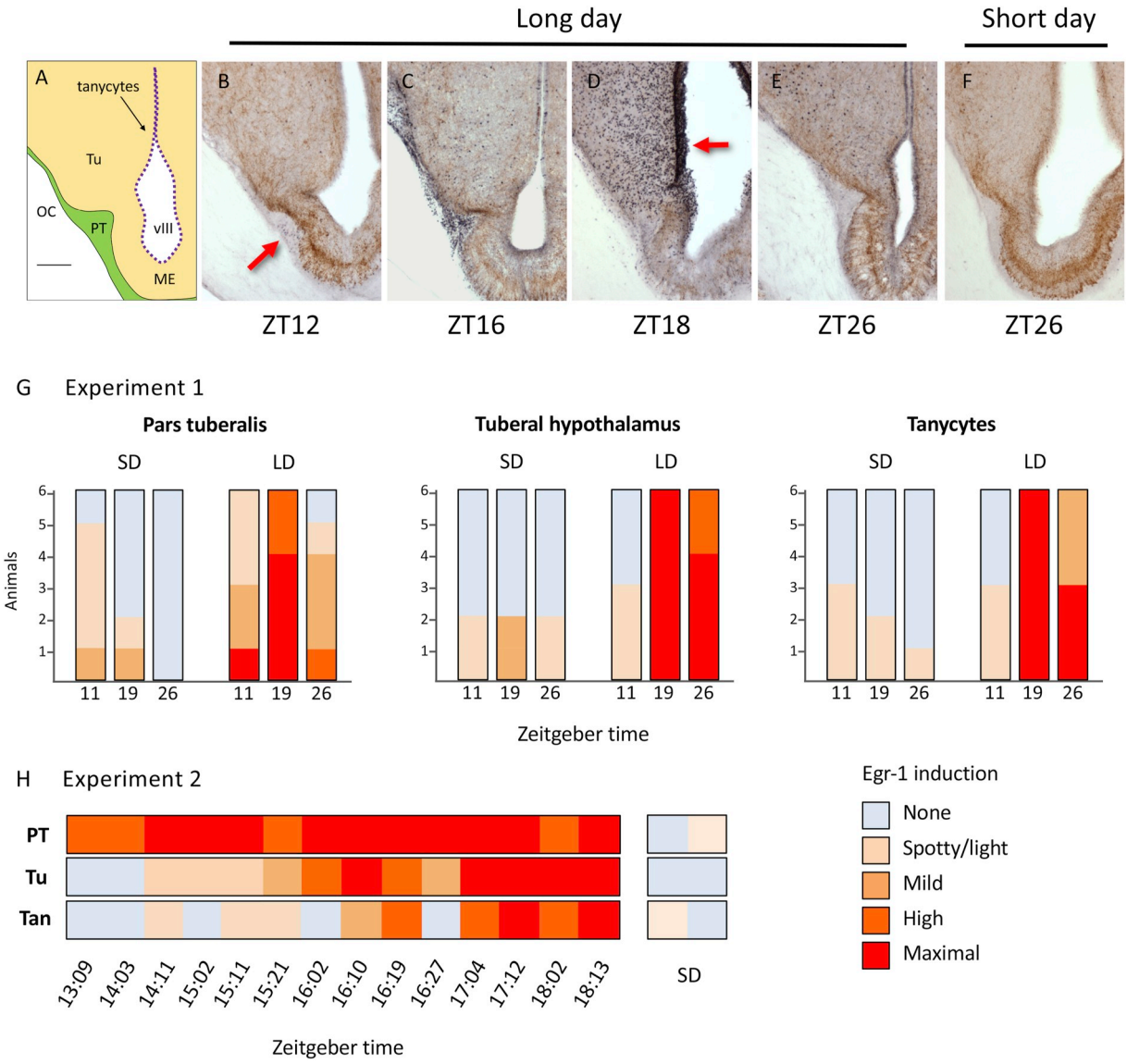

Fig. 3. Induction of Egr-1-ir by a single long day. Images and graphs are arranged to show the effect of Zeitgeber time (ZT), in other words the number of hours since dawn of the first long day. (A) Egr-1-ir was assessed in the pars tuberalis (PT), the tuberal hypothalamus (Tu), which includes the infundibular nucleus, and the tanycytes (ependymal cells) lining the third ventricle (vIII). In (B–F), photomicrographs show Egr-1 induction in four long-day birds and one short-day bird. These sections were double-labeled for TH-IR (brown cells and fibers) and Egr-1-IR (black dots), For this figure, only the Egr-1-ir is relevant. (B) In long day birds, PT (arrow) began to show Egr-1 induction at about ZT11. (C) The labeling in PT was more robust by ZT16, and induction was beginning in Tu. (D) By ZT19, induction in Tu was maximal and the tanycytes lining vIII were also expressing Egr-1-ir (arrow). (E) By ZT26 (ZT2 next day), induction in Tu and the tanycytes was still present, but induction in PT had waned. (F) Low levels of induction were seen in birds that remained on short days. Subjective ratings are plotted in (G) for Egr-1 induction in PT, Tu, and the tanycytes for each group in Experiment 1. The height of each color block represents the number of birds, out of six within each group, exhibiting the corresponding level of Egr-1 induction. LD = long day; SD = short day. The time course of induction in Experiment 2 is shown in (H). The two short-day birds were sampled at ZT18:22 and 18:30. In both experiments, birds were housed in the same environmental chamber with one (Experiment 1) or one to three (Experiment 2) of the other birds; thus, samples are not all independent. ME, median eminence. OC, optic chiasm. ME, median eminence. Scale bar in A = 100 μm, applies to (A-F).

When they did not match, the higher number was used in the analysis. The VIP-IR label was dense in the tuberal hypothalamus but did not interfere with assessment of the Egr-1 induction on this qualitative scale.

2.1.7. Statistical analysis

Analysis of Egr-1 induction in PT, the tuberal hypothalamus, and within GnRH-IR cells was done qualitatively. Analysis of Egr-1 induction within TH-IR and VIP-IR cells was done statistically. Because the number of TH-IR or VIP-IR cells co-expressing Egr-1-ir was sometimes zero, the data on percent colocalization were highly non-normal. We therefore added "1" to both the total number of TH-IR or VIP-IR cells and the number of those cells co-expressing Egr-1-ir. This extra step was not done for VIP-IR cells in PMM, because there were no zeros in that data set. Data for all measures (TH-IR or VIP-IR cell counts and the percent colocalization within each population) were then square-root transformed and analyzed in linear mixed models. We included day-length (LD or SD) and ZT (ZT11, ZT19, or ZT26) as fixed effects. Note that the plumage morphs in this species are defined by a chromosomal rearrangement that affects genes relevant to this study, such as those encoding VIP and opsin 5 (Michopoulos et al., 2007; Zinzow-Kramer et al., 2015). Therefore, plumage morph was included as a fixed effect in these models as well. Each model was full factorial, including all interaction terms for all fixed effects. Chamber was included as a random effect. When we found significant interactions between day-length and ZT, or significant main effects of both, we performed post-

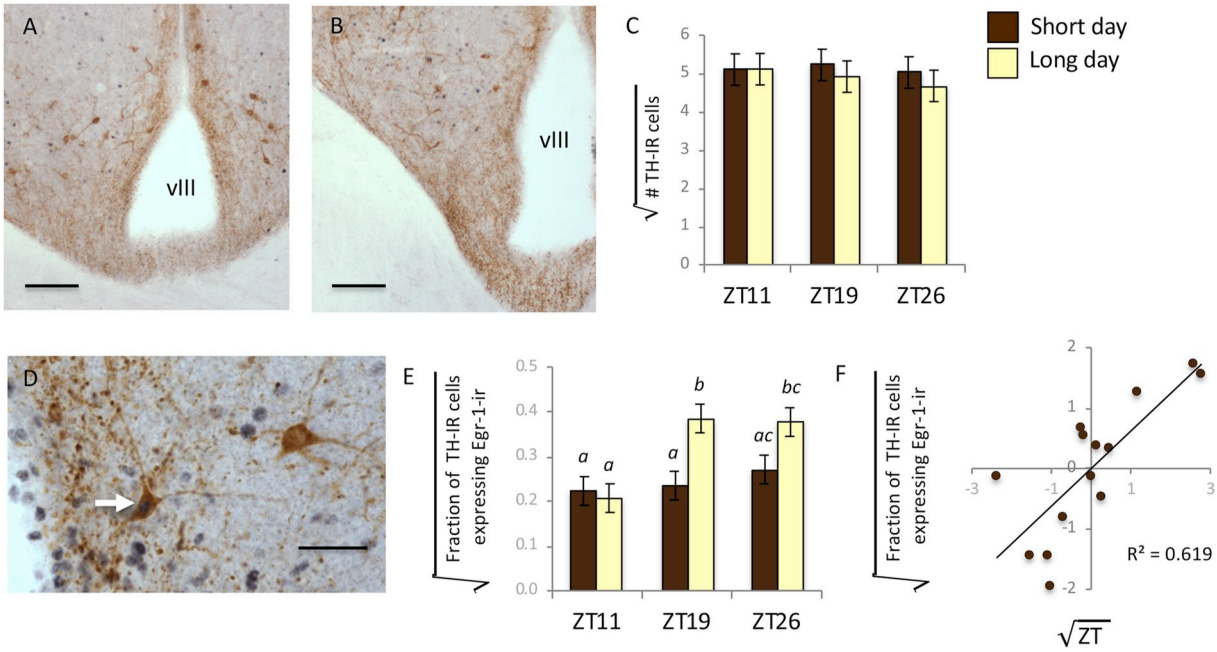

Fig. 4. Effects of photostimulation and Zeitgeber time (ZT) on cells immunoreactive (IR) for tyrosine hydroxylase (TH) in the tuberal hypothalamus. (A, B) TH-IR cells (reddish brown cell bodies) were counted in a region corresponding to the ventral A14/A12 cell group (Reiner et al., 1994), which overlaps with the photo-induced Egr-1 response (see Fig. 3). Photos are shown at two rostro-caudal levels. Scale bar = 100 μm. (C) shows TH-IR cell counts from Experiment 1. Estimated marginal means (EMMs), controlling for plumage morph and chamber, are plotted. $N = 6$ in each of the six groups. In (D), a photomicrograph illustrates an example of colocalization of Egr-1-IR (purplish gray nucleus) and TH-IR (brown soma) (arrow). Scale bar = 25 μm. Long days induced Egr-1-ir in TH-IR cells by ZT19 (E). EMMs are plotted. $N = 6$ in each of the six groups. Columns with different letters represent groups significantly different from each other, across either ZT or day length. (F) In Experiment 2, the percentage of TH-IR cells co-expressing Egr-1-ir increased significantly between ZT13 and ZT18 ($p = 0.002$). The scatterplot shows residuals after controlling for plumage morph and chamber. vIII, third ventricle.

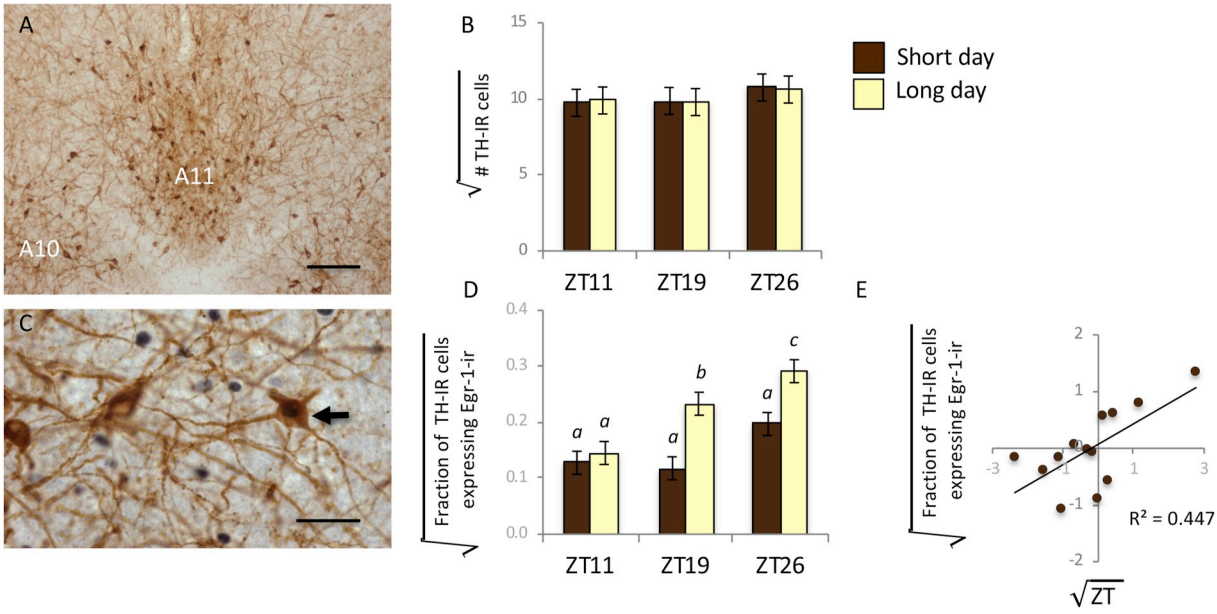

Fig. 5. Effects of photostimulation and Zeitgeber time (ZT) on cells immunoreactive for tyrosine hydroxylase (TH) in the premammillary nucleus (PMM). (A) TH-IR cells were counted in a region corresponding to a portion of the A11 cell group (Kuenzel and Masson, 1988; Reiner et al., 1994). Scale bar = 100 μm. (B) TH-IR cell counts did not change across ZT in Experiment 1 (see Methods). Estimated marginal means (EMMs), controlling for plumage morph and chamber, are plotted. $N = 6$ in each of the six groups. (C) shows an example of colocalization of Egr-1-IR (purplish, dark nucleus) and TH-IR (brown cytoplasm and processes) in this region (arrow). Scale bar = 25 μm. (D) Long days induced Egr-1-ir in TH-IR cells by ZT19. EMMs are plotted. Columns with different letters represent groups significantly different from each other, across either ZT or day length. $N = 6$ in each of the six groups. (E) In Experiment 2, the percentage of TH-IR cells co-expressing Egr-1-ir was positively correlated with ZT between ZT13 and ZT18 ($p = 0.006$). The scatterplot shows residuals after controlling for plumage morph and chamber.

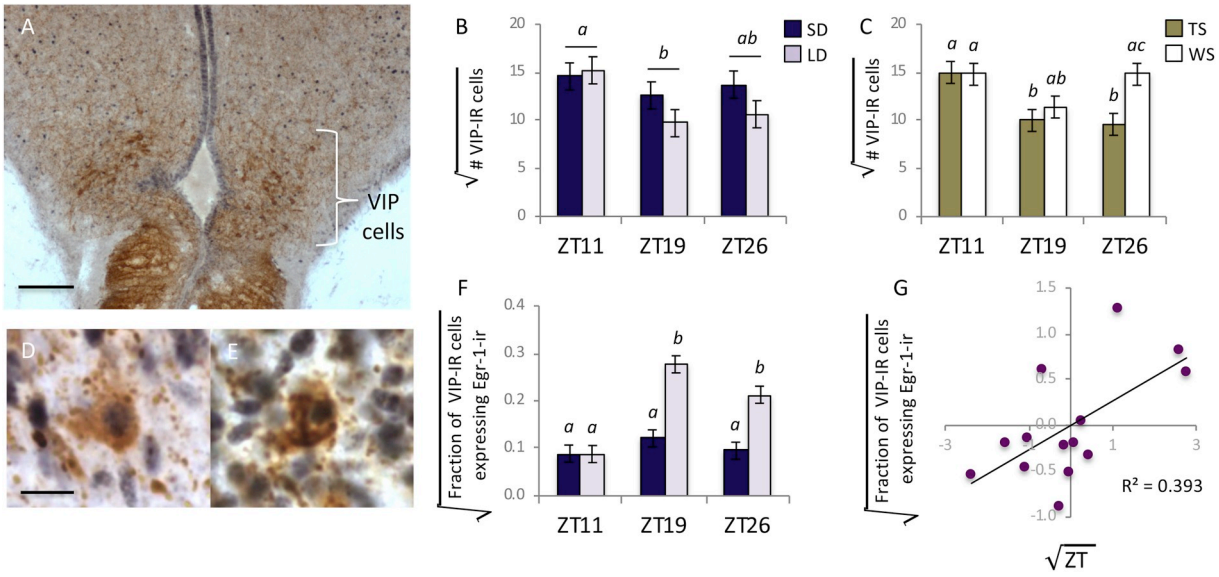

Fig. 6. Effects of photostimulation and Zeitgeber time (ZT) on cells immunoreactive for vasoactive intestinal peptide (VIP) in the tuberal hypothalamus. (A) VIP-IR cells were counted in the tuberal hypothalamus within the infundibular nucleus. (B) shows VIP-IR cell counts at Zeitgeber times (ZT) in Experiment 1 (see Methods) Estimated marginal means, controlling for plumage morph and chamber, are plotted. SD = short day; LD = long day. Columns with different letters depict significant differences between ZT groups. The same data, parsed by plumage morph, are plotted in (C). Columns with different letters represent groups significantly different from each other, across either ZT or morph. $N = 6$ in each of the six groups for both (B) and (C). (D) shows an example of a VIP-IR cell (reddish brown) co-expressing Egr-1 (purplish gray). Such cells were relatively rare. More frequently, we observed Egr1-IR neurons surrounded by basket-like VIP fibers as shown in (E). (F) Long days induced Egr-1-ir in VIP-IR cells by ZT19. EMMs are plotted. Columns with different letters represent groups significantly different from each other, across either ZT or daylength. $N = 6$ in each of the six groups. (G) In Experiment 2, the percentage of VIP-IR cells co-expressing Egr1-IR increased between ZT13 and ZT18 ($p = 0.029$). The scatterplot shows residuals after controlling for plumage morph and chamber. Scale bar in (A) = 100 μm. Scale bar in (D) also applies to (E) = 10 μm.

hoc mixed model analyses to test for effects of daylength within the ZT levels and effects of ZT within the daylength levels. When we found significant effects of ZT only, we used post-hoc mixed models to determine which time points were different from each other, collapsing across daylength. All analyses were performed in SPSS v. 26.

2.2. Experiment 2

2.2.1. Animals and experimental design

Because Experiment 1 showed significant differences in some measures between ZT11 (a group spanning ZT10.5 – ZT12) and ZT19 (spanning ZT18 – ZT19.5), we wanted to parse out the time course of these events with greater resolution. We therefore conducted a follow-up study in which we photostimulated birds with a 16 L:8D day, as in Experiment 1, and sampled them between ZT13.0 and ZT18.5 (Fig. 1). For this experiment, 16 male white-throated sparrows were collected on the campus of Emory University during autumn migration and housed in an aviary in the Emory animal facility on SD (8 L:16D) for 10–12 weeks. In late January they were transferred to individual cages inside walk-in sound-attenuated chambers, two to four birds per chamber. After three days, the light cycle was changed to LD (16 L:8D) for all but two birds. Those two birds remained on SD as a control. The photostimulated birds were sampled at intervals between ZT13 and ZT18.5; the majority was sampled between ZT15 and ZT16.5 (Fig. 1). The two SD birds were sampled at ZT18. All testes were confirmed to be in a regressed state. All procedures for tissue collection, immunohistochemical staining, and cell counting were as described for Experiment 1. The percent Egr-1 in TH neurons in A11 could not be assessed in one bird because of tissue damage in those sections.

2.2.2. Statistical analysis

We tested for correlations between ZT and each variable of interest, in other words variables that appeared to change between ZT11 and ZT19 in Experiment 1. ZT was treated as a continuous variable in partial Pearson correlations, controlling for plumage morph and chamber, in SPSS v. 26. We adjusted alpha for the number of tests using sequential Bonferroni corrections (Rice, 1989).

3. Results

3.1. Experiment 1

3.1.1. Egr-1 induction in GnRH-IR neurons

The distribution of GnRH-IR neurons was similar to that reported by Saab et al. (2010). Colocalization of Egr-1-ir in GnRH-IR neurons was absent from all but one animal, which was sampled at exactly ZT26.0 (ZT2 the following day). In that animal, approximately 50% of the GnRH-IR neurons in the preoptic area were immunopositive for Egr-1 (Fig. 2C). The double-labeled cells were confined to the center of this cell population, where the GnRH-IR neurons are densest (Fig. 2A). The GnRH-IR neurons on the periphery of this population, in the rostral, caudal, lateral, and dorsal directions, were not double-labeled. We detected no colocalization in the remaining five animals in the LD ZT 26 group, each of which was sampled between one and 60 min before the animal with colocalization. Egr-1 labeling was completely absent from GnRH-IR somata in every other brain region, including the nucleus of the pallial commissure and the lateral septal area, in every bird.

3.1.2. Egr-1 induction in PT and the tuberal hypothalamus

We noted striking Egr-1 induction in PT in the LD animals only. Induction in PT appeared to be beginning already by ZT11, was very high at ZT19, and had begun to decrease by ZT26 (Fig. 3). We noted substantial induction of Egr-1 throughout the tuberal hypothalamus in LD animals, particularly in the cells surrounding vIII, which are presumably tanycytes (Fig. 3D and E). This induction was not present at ZT11, but was clear by ZT19 and persisted at ZT26. Similar levels of induction were not seen in SD animals (Fig. 3F).

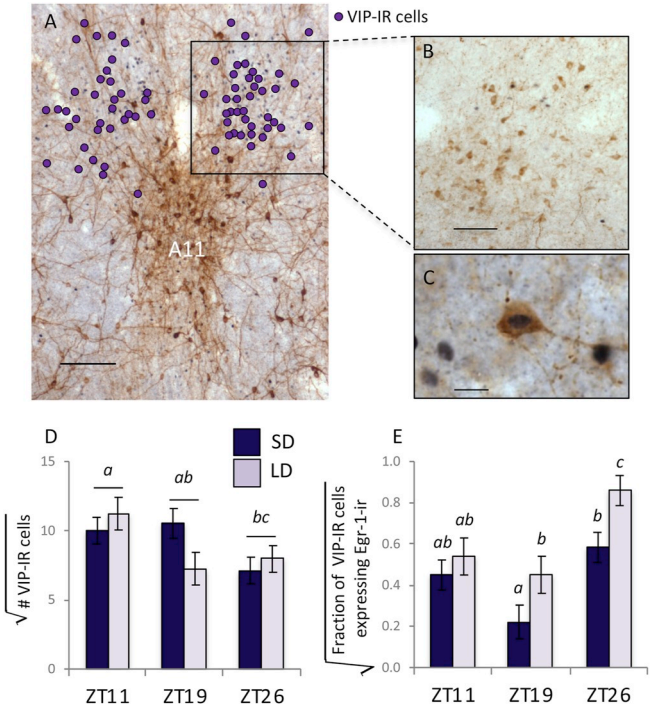

Fig. 7. Effects of photostimulation and Zeitgeber time (ZT) on cells immunoreactive (IR) for vasoactive intestinal peptide (VIP) in the premammillary nucleus (PMM). To make panel (A), a photomicrograph of the dopaminergic A11 cell group, immunolabeled for tyrosine hydroxylase (see Fig. 5) was overlain with a photomicrograph of VIP immunolabeling in an adjacent section from the same bird. The locations of the VIP-IR cells were then marked (purple circles) and the VIP-IR photo removed to reveal the spatial relationship between the two cell groups in this region. (B) shows a different example of VIP-ir in this area. (C) shows an example of a cell co-expressing VIP-ir (reddish brown, in cytoplasm) and Egr-1-ir (purplish gray, in nucleus). (D) shows VIP-IR cell counts at Zeitgeber time (ZT) groups in Experiment 1 (see Methods). SD = short day; LD = long day. Columns with different letters depict significant differences between ZT groups. (E) shows the percentage of VIP-IR cells expressing Egr-1-ir. Columns with different letters represent groups significantly different from each other, across either ZT or daylength. In both (D) and (E), estimated marginal means (EMMs), controlling for plumage morph and chamber, are plotted. $N = 6$ in each of the six groups in both panels. Scale bars: (A) = 100 μm; (B) = 50 μm; (C) = 10 μm.

3.1.3. TH cells

The effects of daylength and ZT on the TH-IR cell populations are shown in Fig. 4 for the tuberal hypothalamus and Fig. 5 for PMM. There were no effects of daylength or ZT group on the number of TH-IR cells, and no interactions, in either region (Table 1). In both regions, both daylength and ZT affected the expression of Egr-1-ir in TH-IR cells (Table 1). The interaction between daylength and ZT was significant for the tuberal hypothalamus and marginal for PMM. In the tuberal hypothalamus, long daylength increased percent colocalization significantly by ZT19 ($p = 0.029$, compared with ZT11) and it was still elevated, relative to ZT11, the following morning at ZT26 ($p < 0.001$). No changes could be detected in SD birds, in which percent colocalization was significantly lower than in LD birds at ZT19 ($p = 0.047$).

In PMM, long daylength increased percent colocalization by ZT19 ($p = 0.035$ compared with ZT11). Percent colocalization in PMM continued to climb, such that levels at ZT26 were even higher than at ZT19 ($p < 0.046$). Not all of this expression could be attributed to long daylength, however, because by ZT26, percent colocalization also increased marginally in the SD birds ($p \sim 0.08$ compared with either ZT11 or ZT19). Thus, some of the colocalization could be due to a circadian rhythm or the lights-on stimulus the following morning, rather than photostimulation. Nonetheless, percent colocalization was higher in LD than SD birds at both ZT19 ($p < 0.013$) and ZT26 ($p = 0.014$).

3.1.4. VIP cells

The effects of daylength and ZT on the number of VIP-IR cells are shown in Fig. 6 for the tuberal hypothalamus and Fig. 7 for PMM. In both regions, there was a main effect of ZT but no effect of daylength and no interaction between the two factors (Table 1). Consistent with Zhao et al. (2018), the number of VIP-IR cells in the tuberal hypothalamus decreased by ZT19 ($p = 0.041$) and remained marginally reduced at ZT26 ($p = 0.054$). Unlike other variables we measured in this study, the number of VIP-IR cells in the tuberal hypothalamus depended on plumage morph (Fig. 6C; $F_{1,12} = 8.274$; $p = 0.014$). The degree to which the number of cells decreased over time also depended on morph ($F_{2,12} = 7.359$; $p = 0.008$), such that the decrease was apparent only in birds of the tan-striped morph (Fig. 6C).

Although we have no evidence that photostimulation per se affected the number of VIP-IR cells in the tuberal hypothalamus, it did affect the percentage of those cells that co-expressed Egr1-ir. Whereas the percent colocalization was very low in both LD and SD birds at ZT11-12, it increased dramatically by ZT19 ($p < 0.001$) in LD birds; at this time point, percent colocalization was higher in LD than SD birds ($p < 0.001$). By ZT26, percent colocalization was still higher than at ZT11 ($p = 0.031$) and higher than in SD birds ($p = 0.032$). We noted that in birds with robust photic responses, the Egr-1 immunopositive cells were sometimes surrounded by VIP-ir fibers, forming baskets (Fig. 6E).

As in the tuberal hypothalamus, the number of VIP-IR cells in PMM

Table 1
Results of univariate F-tests in Experiment 1. Main effects of daylength and Zeitgeber time (ZT) were tested on the numbers of TH-IR or VIP-IR cells in the tuberal hypothalamus (Tu) and the premammillary nucleus (PMM), and the percentage of those cells that co-expressed Egr-1-ir (% colo). Note that in addition to daylength and ZT, plumage morph was included as a fixed factor in all tests; in most cases there were no effects of morph on the dependent variables and no interactions between morph and either other factor ([a]see Results for a single exception). All models included chamber as a random effect. Significant effects are noted in **bold** ($\alpha = 0.05$).

			Daylength		ZT		Daylength X ZT	
			$F_{(df)}$	p	$F_{(df)}$	p	$F_{(df)}$	p
TH	Tu	# cells	$0.412_{(1,12)}$	0.533	$0.227_{(2,12)}$	0.800	$0.196_{(2,12)}$	0.825
		% colo	$9.582_{(1,12)}$	**0.005**	$6.988_{(2,12)}$	**0.004**	$3.680_{(2,12)}$	**0.040**
	PMM	# cells	$0.001_{(1,12)}$	0.982	$0.626_{(2,12)}$	0.551	$0.015_{(2,12)}$	0.985
		% colo	$20.390_{(1,12)}$	**0.001**	$14.082_{(2,12)}$	**0.001**	$3.149_{(2,12)}$	0.080
VIP	Tu	# cells[a]	$2.386_{(1,12)}$	0.148	$3.747_{(2,12)}$	**0.054**	$1.103_{(2,12)}$	0.363
		% colo	$35.158_{(1,12)}$	< **0.001**	$19.043_{(2,12)}$	< **0.001**	$10.308_{(2,12)}$	**0.002**
	PMM	# cells	$0.219_{(1,12)}$	0.645	$4.548_{(2,12)}$	**0.024**	$2.574_{(2,12)}$	0.103
		% colo	$9.103_{(1,11)}$	**0.007**	$12.097_{(2,11)}$	< **0.001**	$0.746_{(2,11)}$	0.488

[a] see Results section 3.1.4 for F and p values for significant effects of plumage morph for this variable.

decreased with increasing ZT, but there was no effect of daylength (Fig. 7D). Post-hoc tests showed that the number of VIP-IR cells in PMM did not decrease significantly by ZT19 ($p = 0.225$) but it did decrease by ZT26 ($p = 0.009$). Although the data gave the appearance that the number of VIP-IR cells may have decreased more quickly in LD birds, we could not detect an interaction between ZT and daylength. We did, however, detect highly significant main effects of both daylength and ZT on the percentage of VIP-IR cells in PMM that co-expressed Egr-1-ir. Percent colocalization was higher in LD than SD birds, an effect that appears to have been driven primarily by birds at the ZT19 and ZT26 time points (Fig. 7E). Percent colocalization was lowest at ZT19 and increased significantly by ZT26 ($p < 0.020$ in both LD and SD birds, compared with ZT19). Because this pattern (a non-significant decrease followed by an increase) was visible in both LD and SD birds, it appeared to be due to a circadian rhythm rather than photostimulation.

3.2. Experiment 2

3.2.1. Egr-1 induction in PT and the tuberal hypothalamus

In Experiment 1, we found that a number of measures changed dramatically between ZT11 and ZT19 (Figs. 3–6). Among these measures were Egr-1 induction in PT and the tuberal hypothalamus, including the tanycytes lining vIII (Fig. 3). In Experiment 2, we sampled birds at intervals between these two time points, starting at ~ ZT13 and ending at ~ ZT18.5 (Fig. 1). PT was already expressing high levels of Egr1-IR in all of these animals, which is consistent with evidence from Experiment 1 suggesting that PT was already responding by ZT11 (Fig. 3G). Thus, the induction in PT preceded the induction in the tuberal hypothalamus, which began at approximately ZT16. Induction in the tanycytes occurred at about the same time or shortly after (Fig. 3H). Overall, these results are consistent with current models in which PT responds first, followed by the tanycytes (reviewed by Nakane and Yoshimura, 2019).

3.2.2. TH cells

In the tuberal hypothalamus, the percentage of TH-IR cells expressing Egr-1 was positively correlated with ZT ($p = 0.002$, $\alpha = 0.013$). The increase appeared to occur gradually over time, without an apparent jump at any particular ZT (Fig. 4F). For PMM the pattern was similar ($p = 0.006$, $\alpha = 0.017$) but with a notable rise after ~ ZT16.5 (Fig. 5E).

3.2.3. VIP cells

The number of VIP-IR cells in the tuberal hypothalamus was weakly negatively correlated with ZT, but not significantly so ($p = 0.405$, $\alpha = 0.05$). Limiting the analysis to just tan-striped birds did not increase the strength of the correlation. The percentage of VIP-IR cells in this region that expressed Egr-1-ir was positively correlated with ZT but only marginally so after correcting for multiple comparisons ($p = 0.029$, $\alpha = 0.025$; Fig. 6G).

4. Discussion

4.1. Photo-induced responses in GnRH neurons

In a previous study of white-throated sparrows in non-breeding condition (Saab et al., 2010), we showed that Egr-1-IR was induced in GnRH neurons by a single long day. In that study, we sampled between two and 3 h after dawn the following day (ZT26.1 at the earliest). Our primary goal in the current study was to determine when, relative to other photo-induced events in the brain, this Egr-1-IR in GnRH neurons was first detectable. Of all 36 birds in Experiment 1, only one showed Egr-1-IR in GnRH neurons – the very last one sampled, at 26.0 h after dawn of the first long day (Fig. 2C). Thus, the induction we observed by ZT26.1 in our original study (Saab et al., 2010) is not likely to have been detectable any earlier.

IEG induction in GnRH cells does not occur concomitantly with release (Meddle and Follett, 1997; Meddle et al., 1999, 2006; Saab et al., 2010); rather, the induction we detected in GnRH somata could be related to new synthesis. New GnRH synthesis is not expected to alter the number of detectable GnRH-IR somata. We did not count GnRH-IR somata in the present study, but in our previous study we did not observe an increase in their number by ZT26-27 (Saab et al., 2010). This finding is consistent with studies in white-crowned sparrows and European starlings (*Sturnus vulgaris*) showing that the number of GnRH neurons does not change even after many days of photostimulation, despite large increases in plasma LH (Meddle et al., 1999; Parry et al., 1997). This lack of obvious increases in GnRH-ir, despite presumed increases in GnRH synthesis, is thought to be due to the copious release occurring during the photostimulated state (Meddle et al., 2006).

4.2. Photo-induced responses in the tuberal hypothalamus

According to current models in birds (reviewed by Nakane and Yoshimura, 2019), the photoperiodic response begins when photoreceptive cells detect light after a certain point in the evening. The identity of those cells, the photopigment they produce, and the exact time of day at which light activates them likely vary among species (García-Fernández et al., 2015; Kang et al., 2010; Perfito et al., 2014; Zhao et al., 2018). Downstream of the photoreceptors, the sequence of events is thought to be similar in birds and mammals (Korf, 2018). The PT begins to secrete TSH, which stimulates production of T3 by the vIII tanycytes. The T3 acts in turn to cause nearby tanycytes to retract their endfeet, allowing GnRH terminals to contact the portal vasculature (reviewed by Nakane and Yoshimura, 2019; Rodríguez-Rodríguez et al., 2019). Our results are consistent with this model. Within the mediobasal hypothalamus we noted the earliest induction of Egr-1 in the PT (Fig. 3), which was higher than baseline levels by ZT12, and quite clear by Z13. This induction clearly preceded that in the tuberal hypothalamus, which began at least 3 h later. The tanycytes lining vIII began expressing Egr-1-ir at high levels between ZT16 and ZT17; we cannot determine here, however, whether this induction lagged behind that of the rest of Tu or whether it occurred concurrently. By ZT26, Egr-1-ir in the tuberal hypothalamus was still maximal but the labeling in PT had begun to wane, and in fact was at baseline levels in several birds at this last time point (Fig. 3). This finding is consistent with the prevailing model of avian photostimulation (e.g., Nakane and Yoshimura, 2019), in which the response in PT is one of the earliest photo-induced events. Here we show that in white-throated sparrows, this response is transient and is no longer striking by the next morning.

The induction of Egr-1 in the tuberal hypothalamus was remarkably dense by ZT18 (Fig. 3D). In order to determine the phenotype of at least some of these cells, we looked for colocalization of Egr-1-ir and either TH-ir or VIP-ir. Only a small fraction of the Egr-1-ir cells in the tuberal hypothalamus co-expressed either antigen. Likewise, only a small fraction of the TH-IR or VIP-IR cells in this region co-expressed Egr-1-ir (Figs. 4–7). Nonetheless, in LD birds we detected an increase in the percentage of TH-IR neurons co-expressing Egr-1-IR (Fig. 4E and F). This induction occurred at about the same time as the rest of the Egr-1 response in the tuberal hypothalamus (Fig. 3). The responding TH-IR cells were located at the boundary between the ventral A14 and A12 dopaminergic cell populations (see Reiner et al., 1994). These cells are thought to project ventrally toward the median eminence and may be involved in regulation of both GnRH (Contijoch et al., 1992) and prolactin (Bhatt et al., 2003; Youngren et al., 1988).

Dopaminergic responses in the tuberal hypothalamus may be directly related to responses in VIP neurons in the same region, which were detectable in this study at roughly the same time (Fig. 6). In turkeys, infusion of dopamine directly into vIII stimulated the expression of VIP mRNA in the infundibular nucleus and increased plasma prolactin within minutes (Bhatt et al., 2003). Note, however, that in turkeys, IEG expression was not induced in VIP neurons by photic cues

(Thayananuphat et al., 2007b) as it was in our study. We also detected a decrease in the number of VIP cells in the region between ZT11 and ZT19 (Fig. 6B), which could be consistent with VIP release; however, this decrease was not associated with daylength. This result is consistent with studies of house sparrows (*Passer domesticus*) and white-crowned sparrows, in which the number of infundibular VIP-IR cells decreased over the course of the day such that fewer cells were detectable at night (Wang and Wingfield, 2011; Zhao et al., 2018).

The function of photo-induced VIP responses is not completely clear. There is some evidence from songbirds and rodents that prolactin, which is stimulated by VIP activity (Maney et al., 1999a), can have pro-gonadal effects early in the breeding season (Bex et al., 1978; Das, 1991; Maney et al., 1999b). Nevertheless, the role of VIP and prolactin in avian photoperiodicity has been discussed largely in the context of photorefractoriness and gonadal regression rather than photostimulation and gonadal recrudescence (Deviche et al., 2000; Sharp, 2005). It is thought that photostimulation sets into motion two separate processes: a rapid one that causes recrudescence and a slower one that ultimately culminates in regression. This second, slower process is hypothesized to involve the VIP/prolactin axis, meaning that the VIP/PRL response to photic cues should occur on a longer time scale compared with the GnRH/LH response (El Halawani et al., 2009; Sharp, 2005). Our data from sparrows do not support this model in that we see Egr-1 induction in VIP cells in the tuberal hypothalamus by ~ ZT17 of the first long day (Fig. 6G). In addition, re-analysis of data from Maney et al. (1999b) shows that in some subspecies of white-crowned sparrow, plasma prolactin increased significantly after a single long day. We must consider the possibility that those observations, as well as those in the current study, were simply an artifact of the 1st long day paradigm. The VIP/prolactin response may, under natural circumstances, occur later in the season because the photoperiodic threshold for its activation is later in the day and therefore is passed at a later date. In other words, the GnRH/LH and VIP/prolactin axes may have two different thresholds for daylength, which are passed on different dates as daylengths gradually increase during the spring. In our artificial paradigm, birds could be exposed to conditions exceeding both thresholds within a few hours. Thus, we may be seeing processes that normally do not co-occur. Alternatively, the two processes may have the same threshold and share neural mechanisms, but the prolactin response lags behind by a few hours or days.

4.3. Photo-induced responses in the premammillary region

In turkeys, the infundibular region of the hypothalamus is relatively devoid of photoperiodic responses during the first long day (Thayananuphat et al., 2007a). Instead, the most robust responses are seen more caudally, in PMM (Thayananuphat et al., 2007a,b). In this region, which corresponds to the dopaminergic A11 cell group, TH-IR neurons co-express not only melatonin but also opsin, meaning that these cells are likely photosensitive (Kang et al., 2010). They express TH-IR in a circadian rhythm, with the highest expression during the day and the lowest at night (Kang et al., 2007). Kang et al. (2010) proposed that in turkeys, photostimulation begins when these PMM cells communicate light information, via dopamine release, to the PT. The PT is then activated to produce TSH. The results of the current study support this model only partially. First, we could not detect a circadian rhythm in TH-ir in PMM (Fig. 5B). There was a suggestion that TH-ir could be higher in the morning, but this effect was not significant. Second, although TH-IR neurons did respond to the long day (Fig. 5D and E), that response became detectable around ZT16-17, several hours *after* the PT response. Thus, we have no evidence that the signal for PT secretion of TSH originates in PMM (see also Moore et al., 2008). Either that signal is coming from a photosensitive area of the brain that we did not look at in this study, or the earliest signal from PMM is transmitted without an Egr-1 response (much like GnRH release).

In this study, a distinctive population of VIP-IR neurons was located immediately dorsolateral to the TH-IR neurons in the PMM (Fig. 7A). Many of these neurons co-expressed Egr-1-IR. This Egr-1 induction was not related to daylength, but it was significantly affected by ZT; there were fewer VIP-IR cells in morning than in evening (Fig. 7D), and more colocalization of Egr-1-ir in the evening than morning (Fig. 7E). The significance of this finding is unclear. This population of VIP neurons is not among those thought to project to the median eminence to regulate prolactin release (Mauro et al., 1989). When considered along with its proximity to the TH-IR cells of PMM, which could be photoreceptive (Kang et al., 2010), the circadian rhythm expressed in this cell group suggests potential for encoding or conveying information about time of day.

4.4. Effects of plumage morph

White-throated sparrows occur in two plumage morphs, tan-striped and white-striped, which are defined by a chromosomal rearrangement (Thorneycroft, 1975; Thomas et al., 2008). The gene for VIP is located inside this rearrangement and is differentiating between the two haplotypes (Michopoulos et al., 2007). We found that VIP-IR differed between the morphs such that in the infundibular nucleus, immunolabeling was greater in white-striped than in tan-striped birds (Fig. 6C). These results replicate our previous finding of a morph difference in VIP-ir in the infundibular region (Maney et al., 2005; c.f. Horton et al., 2020). The difference was attributable to the fact that VIP-ir decreased over time in the tan-striped birds only. This decrease, which occurs independently of photoperiod and has been observed in other passerines (Wingfield and Wada, 2011; Zhao et al., 2018), could be under the control of a mechanism operating only in the tan-striped and not the white-striped birds. This result adds to a growing literature showing that in passerines, VIP-ir in the infundibular nucleus depends on the time of day. Care should be taken in future studies of VIP expression that time-of-day is well-controlled.

4.5. Limitations of this study

There are several limitations of the current study. First, we did not include females. Because of large sex differences in fall migration patterns (Falls and Kopachena, 2010), we did not have access to a sufficient number of females to include sex as a factor in the study. Because females are generally less sensitive to photic cues in captivity than are males (Ball and Ketterson, 2007; Moore, 1983; Saab et al., 2010), we might not have been able to distinguish a biologically relevant sex difference from a captivity-induced artifact. The main measure in the current study, the dramatic induction of Egr-1-ir in the tuberal hypothalamus, was obvious by ZT26 (ZT2 the following day) in all of the females exposed to long days in our previous study (Saab et al., 2010). We have no reason to suspect there are important sex differences in the timing of this response, but of course the current study provides no evidence either way.

The second limitation was that we limited our proxy for “responses” to the induction of Egr-1-ir. Labeling of IEGs, primarily Fos, has been the standard in this field to identify cells responding to photostimulation (Kang et al., 2007; Majumdar et al., 2014; Meddle and Follett, 1997; Meddle et al., 1999, 2006; Saab et al., 2010; Thayananuphat et al., 2007a; b). It is possible, however, that labeling just one IEG does not capture the entirety of the response. The genes for GnRH, VIP, and two dopamine synthetic enzymes, TH and dopa decarboxylase, all contain Egr-1 binding motifs; therefore, Egr-1 potentially regulates their expression (see Supplementary Material). We do not know, however, whether any of these sites are actively used or important for gene transcription.

A third limitation is that we immunolabeled for only three other antigens: GnRH, VIP, and TH. Of the large number of cells in the mediobasal hypothalamus responding to photostimulation in this study, only a small fraction was immunopositive for VIP or TH. Thus, we have

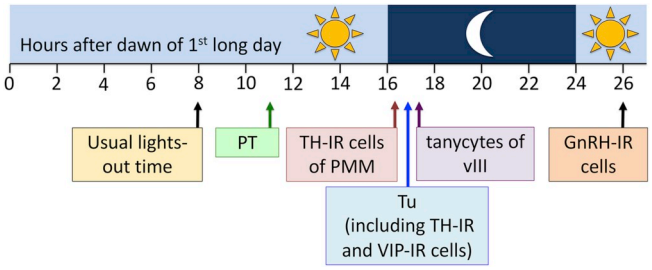

Fig. 8. Timeline of Egr-1 induction observed in this study. We noted induction first in the pars tuberalis (PT) at about Zeitgeber time (ZT) 11. Several hours later, between ZT16 and ZT17, induction was observed in tyrosine hydroxylase (TH) immunoreactive (IR) neurons of the tuberal hypothalamus (Tu) and premammillary nucleus (PMM), in the VIP-IR neurons in PMM, and in the tanycytes lining the third ventricle (vIII). We did not have the temporal resolution necessary in this study to test whether the latter three events occurred at different times or at the same time. Finally, a full 26 h after dawn on the first long day, GnRH-IR neurons began to express Egr-1-IR. This labeling in GnRH-IR cells was noted in only one of six birds sampled between ZT 25 and ZT 26 in the current study (the last bird, sampled at ZT 26.0), but it was observed in eight of eight males sampled between ZT 26.1 and ZT 26.4 by Saab et al. (2010). Together, these two studies suggest that Egr-1 colocalization is observed beginning at ZT 26.

not determined the phenotype of the majority of these responding cells. Research in Japanese quail has shown that many other genes are expressed in the mediobasal hypothalamus during photostimulation, for example DIO2, DIO3, and ICER (Nakao et al., 2008). It is likely that the Egr-1 induction we observed, particularly in the tuberal hypothalamus, occurred in cells of these other phenotypes in addition to VIP-IR and TH-IR neurons.

4.6. Conclusions

Our present data show that in the white-throated sparrow, a highly photoperiodic seasonal breeder, a single long day induces robust Egr-1 responses in the mediobasal hypothalamus. The time course of these responses is summarized in Fig. 8. Egr-1 responses were detected first in PT, at about ZT11, followed a few hours later by responses in tanycytes and in TH-IR and VIP-IR neurons. In contrast, we detected no Egr-1 responses in GnRH neurons until ZT26. These findings are consistent with reports in other species, not only in birds but also sheep and hamsters, in which LH release either preceded IEG responses in GnRH neurons (Doan and Urbanski, 1994; Moenter et al., 1993) or occurred in their absence (Meddle and Follett, 1997; Meddle et al., 1999; Péczely and Kovacs, 2000). Doan and Urbanski (1994) hypothesized that IEG induction in GnRH somata could be induced by new release of sex steroids from the gonads, downstream of LH release. In white-throated sparrows, however, plasma sex steroids are not elevated by ZT26-27 when Egr-1 responses occur in the GnRH neurons (Saab et al., 2010). The GnRH neurons could simply be responding to depletion of GnRH (Doan and Urbanski, 1994) rather than to photic cues per se. Such a model is consistent with the observation that in great tits, photo-induced LH release occurs before an increase in GnRH mRNA (Perfito et al., 2012). Perhaps we should think of the GnRH neuron as a water cooler with a reservoir and a faucet; it is the faucet, which in this case is located in the mediobasal hypothalamus, that responds to photostimulation. The supply of GnRH in the reservoir, in this case the cell bodies in the preoptic area, may be under separate control.

Authors' contributions

DLM, RAA, and KWS conceived and designed the study. DLM and RAA collected the samples. DLM, SEE, and NPJ sectioned the tissue and performed the immunohistochemistry. KWS and DLM analyzed the data. DLM collected the data and drafted the manuscript. All authors provided input on writing the manuscript and approved the final draft.

Funding

This work was funded by NIH 1R01MH082833-01A2 and NSF IOS 0723805 to DLM and NIH NINDS R01NS055125 to KWS. SEE was supported by NIH R25 GM099644. NPJ was supported by NIH R25MH095735-01A1.

Declaration of competing interest

The authors declare no conflicts of interest.

Acknowledgments

The authors wish to thank Katie Barrett, Brent Horton, Chris Goode, Ariella Iancu, Emily Kim, Henry Lange, Camden MacDowell, Jennifer Merritt, Lindsey Rickman, Hillary Rodman, Shelley Parker, Said Saab and Yvonne Eniye for technical assistance. We are grateful to Andreas Fritz for access to his camera for the photomicroscopy. The GnRH antibody was kindly donated by H. Urbanski.

Appendix A. Supplementary material

Supplementary material for this article can be found online at https://doi.org/10.1016/j.mce.2020.110854.

References

Appeltants, D., Ball, G.F., Balthazart, J., 2001. The distribution of tyrosine hydroxylase in the canary brain: demonstration of a specific and sexually dimorphic catecholaminergic innervation of the telencephalic song control nuclei. Cell Tissue Res. 304 (2), 237–259.

Ball, G.F., Ketterson, E.D., 2007. Sex differences in the response to environmental cues regulating seasonal reproduction in birds. Phil. Trans. Biol. Sci. 363 (1490), 231–246.

Ball, G.F., Faris, P.L., Hartman, B.K., Wingfield, J.C., 1988. Immunohistochemical localization of neuropeptides in the vocal control regions of two songbird species. J. Comp. Neurol. 268 (2), 171–180.

Bex, F., Bartke, A., Goldman, B.D., Dalterio, S., 1978. Prolactin, growth hormone, luteinizing hormone receptors, and seasonal changes in testicular activity in the golden hamster. Endocrinology 103, 2069–2080.

Bhatt, R., Youngren, O., Kang, S., El Halawani, M., 2003. Dopamine infusion into the third ventricle increases gene expression of hypothalamic vasoactive intestinal peptide and pituitary prolactin and luteinizing hormone β subunit in the Turkey. Gen. Comp. Endocrinol. 130 (1), 41–47.

Bünning, E., 1960, January. Circadian rhythms and the time measurement in photoperiodism. In: Cold Spring Harbor Symposia on Quantitative Biology, vol. 25. Cold Spring Harbor Laboratory Press, pp. 249–256.

Chaiseha, Y., Youngren, O.M., El Halawani, M.E., 1997. Dopamine receptors influence vasoactive intestinal peptide release from Turkey hypothalamic explants. Neuroendocrinology 65, 423–429.

Contijoch, A.M., Gonzalez, C., Singh, H.N., Malamed, S., Troncoso, S., Advis, J.P., 1992. Dopaminergic regulation of luteinizing hormone-releasing hormone release at the median eminence level: immunocytochemical and physiological evidence in hens. Neuroendocrinology 55 (3), 290–300.

Das, K., 1991. Effects of testosterone propionate, prolactin and photoperiod on feeding behaviours of Indian male weaver birds. Indian J. Exp. Biol. 29, 1104–1108.

Dawson, A., Follett, B.K., Goldsmith, A.R., Nicholls, T.J., 1985. Hypothalamic gonadotrophin-releasing hormone and pituitary and plasma FSH and prolactin during photostimulation and photorefractoriness in intact and thyroidectomized starlings (*Sturnus vulgaris*). J. Endocrinol. 105 (1), 71–77.

Deviche, P., Small, T., 2001. Photoperiodic control of seasonal reproduction: neuroendocrine mechanisms and adaptation. In: Dawson, A., Chaturvedi, C.M. (Eds.), Avian Endocrinology. Narosa Publishing House, New Delhi, pp. 113–128.

Deviche, P., Sabo, J., Sharp, P.J., 2008. Glutamatergic stimulation of luteinising hormone secretion in relatively refractory male songbirds. J. Neuroendocrinol. 20 (10), 1191–1202.

Deviche, P., Saldanha, C.J., Silver, R., 2000. Changes in brain gonadotropin-releasing hormone-and vasoactive intestinal polypeptide-like immunoreactivity accompanying reestablishment of photosensitivity in male dark-eyed juncos (*Junco hyemalis*). Gen. Comp. Endocrinol. 117 (1), 8–19.

Doan, A., Urbanski, H.F., 1994. Diurnal expression of Fos in luteinizing hormone-releasing hormone neurons of Syrian hamsters. Biol. Reprod. 50 (2), 301–308.

Ebling, F.J., Hui, Y., Mirakhur, A., Maywood, E.S., Hastings, M.H., 1993. Photoperiod regulates the LH response to central glutamatergic stimulation in the male Syrian

hamster. J. Neuroendocrinol. 5 (6), 609–618.
El Halawani, M.E., Kang, S.W., Leclerc, B., Kosonsiriluk, S., Chaiseha, Y., 2009. Dopamine–melatonin neurons in the avian hypothalamus and their role as photoperiodic clocks. Gen. Comp. Endocrinol. 163 (1–2), 123–127.
Falls, J.B., Kopachena, J.G., 2010. White-throated sparrow (Zonotrichia albicollis), version 2.0. In: Poole, A.F. (Ed.), The Birds of North America. Cornell Lab of Ornithology, Ithaca, NY, USA.
Follett, B.K., Mattocks, P.W., Farner, D.S., 1974. Circadian function in the photoperiodic induction of gonadotropin secretion in the white-crowned sparrow, *Zonotrichia leucophrys gambelii*. Proc. Natl. Acad. Sci. Unit. States Am. 71 (5), 1666–1669.
Foster, R.G., Plowman, G., Goldsmith, A.R., Follett, B.K., 1987. Immunohistochemical demonstration of marked changes in the LHRH system of photosensitive and photorefractory European starlings (*Sturnus vulgaris*). J. Endocrinol. 115 (2), 211–NP.
García-Fernández, J.M., Cernuda-Cernuda, R., Davies, W.I., Rodgers, J., Turton, M., Peirson, S.N., Foster, R.G., 2015. The hypothalamic photoreceptors regulating seasonal reproduction in birds: a prime role for VA opsin. Front. Neuroendocrinol. 37, 13–28.
Griffiths, R., Double, M.C., Orr, K., Dawson, R.J., 1998. A DNA test to sex most birds. Mol. Ecol. 7 (8), 1071–1075.
Hanon, E.A., Lincoln, G.A., Fustin, J.M., Dardente, H., Masson-Pévet, M., Morgan, P.J., Hazlerigg, D.G., 2008. Ancestral TSH mechanism signals summer in a photoperiodic mammal. Curr. Biol. 18 (15), 1147–1152.
Hiatt, E.S., Goldsmith, A.R., Farner, D.S., 1987. Plasma levels of prolactin and gonadotropins during the reproductive cycle of white-crowned sparrows (*Zonotrichia leucophrys*). Auk 104, 208–217.
Horton, B.M., Moore, I.T., Maney, D.L., 2014. New insights into the hormonal and behavioural correlates of polymorphism in white-throated sparrows. Anim. Behav. 93, 207–219.
Horton, B.M., Michael, C.M., Prichard, M.R., Maney, D.L., 2020. Vasoactive intestinal peptide as a mediator of the effects of a supergene on social behavior. In: Proceedings of the Royal Society B. 287 20200196.
Kabelik, D., Schrock, S.E., Ayres, L.C., Goodson, J.L., 2011. Estrogenic regulation of dopaminergic neurons in the opportunistically breeding zebra finch. Gen. Comp. Endocrinol. 173 (1), 96–104.
Kang, S.W., Leclerc, B., Kosonsiriluk, S., Mauro, L.J., Iwasawa, A., El Halawani, M.E., 2010. Melanopsin expression in dopamine-melatonin neurons of the premammillary nucleus of the hypothalamus and seasonal reproduction in birds. Neuroscience 170 (1), 200–213.
Kang, S.W., Thayananuphat, A., Bakken, T., El Halawani, M.E., 2007. Dopamine-melatonin neurons in the avian hypothalamus controlling seasonal reproduction. Neuroscience 150 (1), 223–233.
Korf, H.W., 2018. Signaling pathways to and from the hypophysial pars tuberalis, an important center for the control of seasonal rhythms. Gen. Comp. Endocrinol. 258, 236–243.
Kuenzel, W.J., Masson, M., 1988. A Stereotaxic Atlas of the Chick (*Gallus domesticus*). Johns Hopkins University Press, Baltimore .
Lake, J.I., Lange, H.S., O'Brien, S., Sanford, S.E., Maney, D.L., 2008. Activity of the hypothalamic-pituitary-gonadal axis differs between behavioral phenotypes in female white-throated sparrows (*Zonotrichia albicollis*). Gen. Comp. Endocrinol. 156, 426–433.
LeBlanc, M.M., Goode, C.T., MacDougall-Shackleton, E.A., Maney, D.L., 2007. Estradiol modulates brainstem catecholaminergic cell groups and projections to the auditory forebrain in a female songbird. Brain Res. 1171, 93–103.
Leclerc, B., Kang, S.W., Mauro, L.J., Kosonsiriluk, S., Chaiseha, Y., El Halawani, M.E., 2010. Photoperiodic modulation of clock gene expression in the avian premammillary nucleus. J. Neuroendocrinol. 22 (2), 119–128.
Lee, W.S., Abbud, R., Hoffman, G.E., Smith, M.S., 1993. Effects of N-methyl-D-aspartate receptor activation on cFos expression in luteinizing hormone-releasing hormone neurons in female rats. Endocrinology 133 (5), 2248–2254.
Li, H., Kuenzel, W.J., 2008. A possible neural cascade involving the photoneuroendocrine system (PNES) responsible for regulating gonadal development in an avian species, *Gallus gallus*. Brain Res. Bull. 76 (6), 586–596.
Macnamee, M.C., Sharp, P.J., Lea, R.W., Sterling, R.J., Harvey, S., 1986. Evidence that vasoactive intestinal polypeptide is a physiological prolactin-releasing factor in the bantam hen. Gen. Comp. Endocrinol. 62, 470–478.
Majumdar, G., Yadav, G., Rani, S., Kumar, V., 2014. A photoperiodic molecular response in migratory redheaded bunting exposed to a single long day. Gen. Comp. Endocrinol. 204, 104–113.
Maney, D.L., Goode, C.T., Lange, H.S., Sanford, S.E., Solomon, B.L., 2008. Estradiol modulates neural responses to song in a seasonal songbird. J. Comp. Neurol. 511, 173–186.
Maney, D.L., Goode, C.T., Lake, J.I., Lange, H.L., O'Brien, S., 2007. Rapid neuroendocrine responses to auditory courtship signals. Endocrinology 148, 5614–5623.
Maney, D.L., Erwin, K.L., Goode, C.T., 2005. Neuroendocrine correlates of behavioral polymorphism in white-throated sparrows. Horm. Behav. 48, 196–206.
Maney, D.L., Schoech, S.J., Sharp, P.J., Wingfield, J.C., 1999a. Effects of vasoactive intestinal peptide on prolactin in passerines. Gen. Comp. Endocrinol. 113, 323–330.
Maney, D.L., Hahn, T.P., Schoech, S.J., Sharp, P.J., Morton, M.L., Wingfield, J.C., 1999b. Effects of ambient temperature on photo-induced prolactin secretion in three subspecies of white-crowned sparrow, *Zonotrichia leucophrys*. Gen. Comp. Endocrinol. 113, 445–456.
Matragrano, L.L., Sanford, S.E., Salvante, K.G., Sockman, K.W., Maney, D.L., 2011. Estradiol-dependent catecholaminergic innervation of auditory areas in a seasonally breeding songbird. Eur. J. Neurosci. 34, 416–425.
Mauro, L.J., Elde, R.P., Youngren, O.M., Phillips, R.E., El Halawani, M.E., 1989. Alterations in hypothalamic vasoactive intestinal peptide-like immunoreactivity are associated with reproduction and prolactin release in the female Turkey. Endocrinology 125 (4), 1795–1804.
Meddle, S.L., Follett, B.K., 1997. Photoperiodically driven changes in Fos expression within the basal tuberal hypothalamus and median eminence of Japanese quail. J. Neurosci. 17 (22), 8909–8918.
Meddle, S.L., Bush, S., Sharp, P.J., Millar, R.P., Wingfield, J.C., 2006. Hypothalamic pro-GnRH-GAP, GnRH-I and GnRH-II during the onset of photorefractoriness in the white-crowned sparrow (*Zonotrichia leucophrys gambelii*). J. Neuroendocrinol. 18 (3), 217–226.
Meddle, S.L., Maney, D.L., Wingfield, J.C., 1999. Effects of N-methyl-D-aspartate on luteinizing hormone release and fos-like immunoreactivity in the male white-crowned sparrow (*Zonotrichia leucophrys gambelii*). Endocrinology 140, 5922–5928.
Michopoulos, V., Maney, D.L., Morehouse, C.B., Thomas, J.W., 2007. A genotyping assay to determine plumage morph in the white-throated sparrow, *Zonotrichia albicollis*. Auk 124, 1330–1335.
Moenter, S.M., Karsch, F.J., Lehman, M.N., 1993. Fos expression during the estradiol-induced gonadotropin-releasing hormone (GnRH) surge of the Ewe: induction in GnRH and other neurons. Endocrinology 133 (2), 896–903.
Moore, A.F., Cassone, V.M., Alloway, K.D., Bartell, P.A., 2018. The premammillary nucleus of the hypothalamus is not necessary for photoperiodic timekeeping in female turkeys (*Meleagris gallopavo*). PloS One 13 (2), e0190274.
Moore, M.C., 1983. Effect of female sexual displays on the endocrine physiology and behaviour of male white-crowned sparrows, *Zonotrichia leucophrys*. J. Zool. 199 (2), 137–148.
Nakane, Y., Yoshimura, T., 2019. Photoperiodic regulation of reproduction in vertebrates. Annu. Rev. Animal Biosci. 7, 173–194.
Nakao, N., Ono, H., Yamamura, T., Anraku, T., Takagi, T., Higashi, K., et al., 2008. Thyrotrophin in the pars tuberalis triggers photoperiodic response. Nature 452, 317–322.
Nicholls, T.J., Follett, B.K., 1974. The photoperiodic control of reproduction in *Coturnix* quail. The temporal pattern of LH Secretion. J. Comp. Physiol. 93 (4), 301–313.
Parry, D.M., Goldsmith, A.R., Millar, R.P., Glennie, L.M., 1997. Immunocytochemical localization of GnRH precursor in the hypothalamus of European starlings during sexual maturation and photorefractoriness. J. Neuroendocrinol. 9, 235–243.
Péczely, P., Kovács, K.J., 2000. Photostimulation affects gonadotropin-releasing hormone immunoreactivity and activates a distinct neuron population in the hypothalamus of the mallard. Neurosci. Lett. 290 (3), 205–208.
Pérez, J.H., Tolla, E., Dunn, I.C., Meddle, S.L., Stevenson, T.J., 2018. A comparative perspective on extra-retinal photoreception. Trends Endocrinol. Metabol. 30, 39–53.
Perfito, N., Jeong, S.Y., Silverin, B., Calisi, R.M., Bentley, G.E., Hau, M., 2012. Anticipating spring: wild populations of great tits (*Parus major*) differ in expression of key genes for photoperiodic time measurement. PloS One 7 (4), e34997.
Reiner, A., Karle, D.J., Adderson, K.D., Medina, L., 1994. Catecholaminergic perikarya and fibers in the avian nervous system. In: Smeets, W.J.A.J., Reiner, A.J. (Eds.), Phylogeny and Development of Catecholamine Systems in the CNS of Vertebrates. Cambridge University Press, Cambridge, pp. 135–181.
Rice, W.R., 1989. Analyzing tables of statistical tests. Evolution 43 (1), 223–225.
Roberts, T.F., Cookson, K.K., Heaton, K.J., Hall, W.S., Brauth, S.E., 2001. Distribution of tyrosine hydroxylase-containing neurons and fibers in the brain of the budgerigar (*Melopsittacus undulatus*): general patterns and labeling in vocal control nuclei. J. Comp. Neurol. 429 (3), 436–454.
Rodríguez-Rodríguez, A., Lazcano, I., Sánchez-Jaramillo, E., Uribe, R.M., Jaimes-Hoy, L., Joseph-Bravo, P., Charli, J.L., 2019. Tanycytes and the control of thyrotropin-releasing hormone flux into portal capillaries. Front. Endocrinol. 10, 401.
Saab, S.S., Lange, H.S., Maney, D.L., 2010. Gonadotropin-releasing hormone neurones in a photoperiodic songbird express Fos and Egr-1 protein after a single long day. J. Neuroendocrinol. 22, 196–207.
Saldanha, C.J., Deviche, P.J., Silver, R., 1994. Increased VIP and decreased GnRH expression in photorefractory dark-eyed juncos (*Junco hyemalis*). Gen. Comp. Endocrinol. 93 (1), 128–136.
Saper, C.B., Sawchenko, P.E., 2003. Magic peptides, magic antibodies: Guidelines for appropriate controls for immunohistochemistry. J. Comp. Neurol. 465, 161–163.
Sharp, P.J., 2005. Photoperiodic regulation of seasonal breeding in birds. Ann. N. Y. Acad. Sci. 1040 (1), 189–199.
Stevenson, T.J., Hahn, T.P., MacDougall-Shackleton, S.A., Ball, G.F., 2012. Gonadotropin-releasing hormone plasticity: a comparative perspective. Frontiers in Neuroendocrinology 33 (3), 287–300.
Thayananuphat, A., Kang, S.W., Bakken, T., Millam, J.R., El Halawani, M.E., 2007a. Rhythm-dependent light induction of the c-fos gene in the Turkey hypothalamus. J. Neuroendocrinol. 19 (6), 407–417.
Thayananuphat, A., Kang, S.W., Bakken, T., Millam, J.R., El Halawani, M.E., 2007b. Rhythmic dependent light induction of gonadotrophin-releasing hormone-I expression and activation of dopaminergic neurones within the premammillary nucleus of the Turkey hypothalamus. J. Neuroendocrinol. 19 (6), 399–406.
Thomas, J.W., Cáceres, M., Lowman, J.J., Morehouse, C.B., Short, M.E., Baldwin, E.L., Maney, D.L., Martin, C.L., 2008. The chromosomal polymorphism linked to variation in social behavior in the white-throated sparrow (*Zonotrichia albicollis*) is a complex rearrangement and suppressor of recombination. Genetics 179, 1455–1468.
Thorneycroft, H.B., 1975. A cytogenetic study of the white-throated sparrow, *Zonotrichia albicollis (Gmelin)*. Evolution 29, 611–621.
Wang, G., Wingfield, J.C., 2011. Immunocytochemical study of rhodopsin-containing putative encephalic photoreceptors in house sparrow, Passer domesticus. Gen. Comp. Endocrinol. 170 (3), 589–596.
Wingfield, J.C., Kenagy, G.J., 1991. Natural regulation of reproductive cycles. Vertebr. Endocrinol.: Fund. Biomed. Implic. 4 (Part B), 181–241 Academic Press.
Yasuo, S., Watanabe, M., Okabayashi, N., Ebihara, S., Yoshimura, T., 2003. Circadian

clock genes and photoperiodism: comprehensive analysis of clock gene expression in the mediobasal hypothalamus, the suprachiasmatic nucleus, and the pineal gland of Japanese quail under various light schedules. Endocrinology 144 (9), 3742–3748.
Youngren, O.M., Chaiseha, Y., El Halawani, M.E., 1998. Regulation of prolactin secretion by dopamine and vasoactive intestinal peptide at the level of the pituitary in the turkey. Neuroendocrinology 68 (5), 319–325.
Zhao, H., Jiang, J., Wang, G., Le, C., Wingfield, J.C., 2018. Daily, circadian and seasonal changes of rhodopsin-like encephalic photoreceptor and its involvement in mediating photoperiodic responses of Gambel's white-crowned Sparrow, *Zonotrichia leucophrys gambelii*. Brain Res. 1687, 104–116.
Zinzow-Kramer, W.M., Horton, B.M., McKee, C.D., Michaud, J.M., Tharp, G.K., Thomas, J.W., Tuttle, E.M., Yi, S.V., Maney, D.L., 2015. Genes located in a chromosomal inversion are correlated with territorial song in white-throated sparrows. Gene Brain Behav. 14, 641–654.